

## Solvent Reorganization Controls the Rate of Proton Transfer from Neat Alcohol Solvents to Singlet Diphenylcarbene

Jorge Peon,<sup>†</sup> Dmitrii Polshakov, and Bern Kohler\**Contribution from the Department of Chemistry, The Ohio State University, 100 West 18th Avenue, Columbus, Ohio 43210*

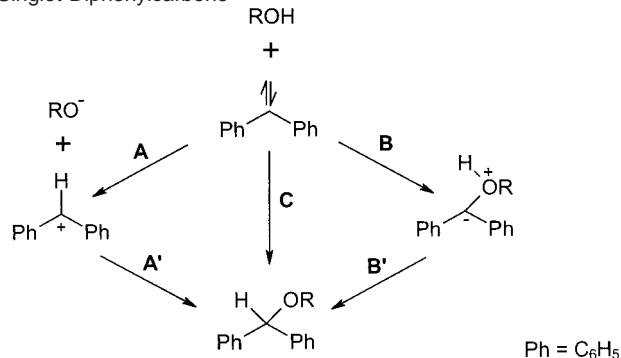
Received November 7, 2001

**Abstract:** Femtosecond transient absorption spectroscopy was used to study singlet diphenylcarbene generated by photodissociation of diphenyldiazomethane with a UV pulse at 266 nm. Absorption by singlet diphenylcarbene was detected and characterized for the first time. Similar band shapes were observed in acetonitrile and in cyclohexane with  $\lambda_{\text{max}} \approx 370$  nm. The singlet absorption decays by intersystem crossing to triplet diphenylcarbene at rates that agree with previous measurements. The singlet absorption band is completely formed 1 ps after the pump pulse. It is preceded by a strong and broad absorption band, which is tentatively assigned to excited-state absorption by a singlet diazo excited state. In neat alcohol solvents the growth and decay of the diphenylmethyl cation was observed. This species is formed by proton transfer from an alcohol molecule to singlet diphenylcarbene. Since a shell of solvent molecules surrounds each nascent carbene, the intrinsic rate of protonation in the absence of diffusion could be measured. In methanol, proton transfer occurs with a time constant of 9.0 ps, making this the fastest known intermolecular proton-transfer reaction to carbon. In O-deuterated methanol proton transfer occurs in 15.0 ps. Slower rates were observed in the longer alcohols. The protonation times correlate reasonably well with solvation times in these alcohols, suggesting that solvent fluctuations are the rate-limiting step. In all alcohols studied, the carbocations decay on a somewhat slower time scale to yield diphenylalkyl ethers. In methanol and ethanol the rate of decay is determined by reaction with neutral solvent nucleophiles. There is evidence in 2-propanol that geminate reaction within the initial ion pair is faster than reaction with solvent. No isotope effect was observed for the reaction of the diphenylmethyl carbocation in methanol. Using comparative actinometry the quantum yield of protonation was measured. In methanol, the quantum yield of carbocations reaches a maximum value of 0.18 approximately 18 ps after the pump pulse. According to our analysis, 30% of the photoexcited diazo precursor molecules are eventually protonated. Somewhat lower protonation efficiencies are observed in the other alcohols. Because the primary quantum yield for formation of singlet diphenylcarbene is still unknown, the importance of reaction channels that might exist in addition to protonation cannot be determined at present. Singlet carbenes are powerful, photogenerated bases that open new possibilities for fundamental studies of proton transfer in solution.

### Introduction

Diphenylcarbene, the simplest diaryl carbene, is a widely studied model system for understanding the spin-dependent reactivity of carbenes.<sup>1</sup> The lowest energy state of diphenylcarbene ( $^3\text{Ph}_2\text{C}$ ) has triplet spin and is 4–5 kcal mol<sup>-1</sup> lower in energy than the lowest singlet state ( $^1\text{Ph}_2\text{C}$ ). Despite their energetic proximity, these two spin states undergo markedly different reactions.  $^3\text{Ph}_2\text{C}$  abstracts hydrogen to produce triplet-polarized radical pairs, while  $^1\text{Ph}_2\text{C}$  inserts into O–H bonds of alcohols to form diphenylalkyl ethers. The mechanism of this reaction has intrigued chemists for over 40 years. Scheme 1 summarizes the reactive pathways, which have been proposed.

**Scheme 1.** Proposed Reaction Pathways for O–H Insertion by Singlet Diphenylcarbene



Protonation to yield diphenylmethyl cation ( $\text{Ph}_2\text{CH}^+$ ) and an alkoxide ion is shown by pathway A. Nucleophilic attack on the carbocation by the geminate alkoxide ion (pathway A') or by a second alcohol molecule (not shown in Scheme 1) then yields the ether product. Alternatively, electrophilic attack by

\* Corresponding author. Telephone: (614) 688-3944. E-mail: kohler@chemistry.ohio-state.edu.

<sup>†</sup> Current address: Arthur Amos Noyes Laboratory of Chemical Physics, California Institute of Technology, Pasadena, CA 91125.

(1) For a review, see: Platz, M. S.; Maloney, V. M. In *Kinetics and Spectroscopy of Carbenes and Biradicals*; Platz, M. S., Ed.; Plenum Press: New York, 1990; pp 239–352.

$^1\text{Ph}_2\text{C}$  on an alcohol molecule can produce an intermediate ylide (pathway B), followed by a 1,2-proton shift (pathway B'). A third possibility is a concerted pathway (pathway C).

A decade ago, Kirmse et al. provided direct spectroscopic evidence for the intermediacy of carbocations in reactions of singlet diarylcarbenes with proton donors.<sup>2</sup> Carbocation intermediates have since been observed for reactions between a number of carbenes and proton donors.<sup>3–5</sup> Although these studies have provided strong evidence in favor of pathway A in Scheme 1, it has been suggested that protonation is only a minor reaction channel.<sup>6,7</sup> In this report, we present new insights into the O–H insertion reaction of  $^1\text{Ph}_2\text{C}$ , which have been obtained by femtosecond transient absorption spectroscopy. As we have shown previously,<sup>8</sup> the femtosecond pump–probe technique allows us to detect even extremely short-lived singlet carbenes.

The fact that carbenes can deprotonate weak proton donors such as alcohols reveals their highly basic character. The gas-phase proton affinity of  $^3\text{Ph}_2\text{C}$  was calculated to be 1151 kJ mol<sup>-1</sup>.<sup>9</sup> Pezacki argued that proton transfer to carbenes is an intrinsically fast reaction akin to those of normal acids and bases.<sup>10</sup> More kinetic data are required to understand the proton-transfer dynamics of these unusual carbon bases. Hence, a second interest in this system is the information it provides about fundamental aspects of proton-transfer reactions in solution. Excitation of  $\text{Ph}_2\text{CN}_2$  with a femtosecond UV pulse generates a powerful base on a subpicosecond time scale. Through spectroscopic detection of  $^1\text{Ph}_2\text{C}$ , we have succeeded in directly measuring the rate of protonation of  $^1\text{Ph}_2\text{C}$  in several neat alcohols for the first time. This has allowed us to study proton-transfer reactions between the solvent and  $^1\text{Ph}_2\text{C}$  in the absence of diffusion. Our results show that  $^1\text{Ph}_2\text{C}$  protonation is among the fastest intermolecular proton-transfer reactions known. Furthermore, the rate of this reaction appears to be controlled by the time required for solvent reorganization.

## Experimental Section

**(1) Spectrometer.** UV pump pulses ( $\lambda = 266$  nm) were obtained by third harmonic generation using a kilohertz-repetition-rate, regeneratively amplified Ti:sapphire laser system. A description of this instrument and the relevant signal acquisition techniques is available elsewhere.<sup>11–13</sup> Probe pulses between 400 and 750 nm were generated by focusing the laser fundamental in a water cell, while probe pulses from 320 to 380 nm were generated in a 1 mm  $\text{CaF}_2$  window with the laser second harmonic. Polarizations of the pump and probe pulses were set to the magic angle. After the sample, the probe beam was passed through an  $f = 0.25$  m monochromator to isolate an approximately 10 nm portion of the continuum for single wavelength measurements. Transient spectra were recorded by scanning the monochromator

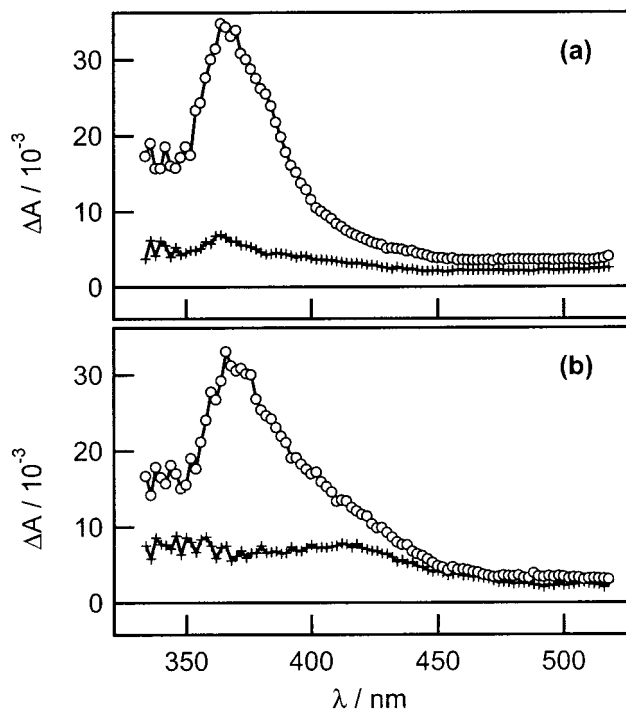


**Figure 1.** Transient spectra observed 30 ps (open circles) and 650 ps (crosses) after photolysis of diphenyldiazomethane with a 180 fs, 266 nm laser pulse in (a) acetonitrile and (b) cyclohexane. The absorption band with  $\lambda_{\text{max}} \approx 370$  nm at 30 ps is assigned to  $^1\text{Ph}_2\text{C}$ .

wavelength. Since the total group delay between the shortest and the longest wavelengths of the continuum is about 2 ps, it was not necessary to apply group delay (“chirp”) correction to transient spectra recorded at delay times greater than approximately 10 ps, as all rapid spectral evolution has ceased by this time. The instrument response was approximately 220 fs (Gaussian full width at half-maximum (fwhm)) as determined by difference frequency mixing between the third harmonic and 10 nm portions of the continuum in a thin BBO crystal.

**(2) Materials.** Diphenyldiazomethane was a generous gift from Professor Matthew S. Platz of our department. The highest purity solvents were obtained from Burdick and Jackson. Deuterated methanol ( $\text{CH}_3\text{OD}$ , 99.5% atom purity) was purchased from Aldrich. All solvents were used as received. Approximately 1 mM solutions were studied in a free flowing jet 0.4 mm thick. Because the diazo compound is continuously photolyzed during the experiments, a large, 0.5 L reservoir was used for recirculating the solutions through the jet. During data acquisition, small samples of the solution were periodically withdrawn and UV/vis absorption spectra were recorded. Solutions were replaced when these spectra indicated significant depletion of the diazo compound.

## Results

### (1) Spectroscopic Detection of Singlet Diphenylcarbene.

A strong transient absorption band ( $\lambda_{\text{max}} \approx 370$  nm) was observed 30 ps after excitation of diphenyldiazomethane ( $\text{Ph}_2\text{CN}_2$ ) by a 150 fs, 266 nm laser pulse in acetonitrile and in cyclohexane (Figure 1). Single-wavelength transients recorded in acetonitrile (Figure 2) and cyclohexane (Figure 3) show the spectral evolution of this band and reveal additional dynamical features. In both solvents, a spikelike transient absorption signal is observed at all probe wavelengths near zero delay time ( $t = 0$ ). This feature shows an instrument-limited rise, followed by a decay with a time constant of  $\approx 300$  fs. An analogous feature was seen in measurements on  $\text{Ph}_2\text{CN}_2$  in methanol (see inset to Figure 6). This subpicosecond decay is intrinsic to diphenyl-

- (2) Kirmse, W.; Kilian, J.; Steenken, S. *J. Am. Chem. Soc.* **1990**, *112*, 6399.
- (3) Chateaufneuf, J. E. *J. Chem. Soc., Chem. Commun.* **1991**, 1437.
- (4) Dix, E. J.; Goodman, J. L. *J. Phys. Chem.* **1994**, *98*, 12609.
- (5) Steenken, S. *Pure Appl. Chem.* **1998**, *70*, 2031.
- (6) Belt, S. T.; Bohne, C.; Charette, G.; Sugamori, S. E.; Scaiano, J. C. *J. Am. Chem. Soc.* **1993**, *115*, 2200.
- (7) Pliego, J. R., Jr.; De Almeida, W. B. *J. Phys. Chem. A* **1999**, *103*, 3904.
- (8) Hess, G. C.; Kohler, B.; Likhovtorik, I.; Peon, J.; Platz, M. S. *J. Am. Chem. Soc.* **2000**, *122*, 8087.
- (9) Pliego, J. R.; DeAlmeida, W. B. *J. Chem. Soc., Faraday Trans.* **1997**, *93*, 1881.
- (10) Pezacki, J. P. *Can. J. Chem.* **1999**, *77*, 1230.
- (11) Peon, J.; Hess, G. C.; Pecourt, J.-M. L.; Yuzawa, T.; Kohler, B. *J. Phys. Chem. A* **1999**, *103*, 2460.
- (12) Peon, J.; Tan, X.; Hoerner, J. D.; Xia, C.; Luk, Y. F.; Kohler, B. *J. Phys. Chem. A* **2001**, *105*, 5768.
- (13) Pecourt, J.-M. L.; Peon, J.; Kohler, B. *J. Am. Chem. Soc.* **2001**, *123*, 10370.

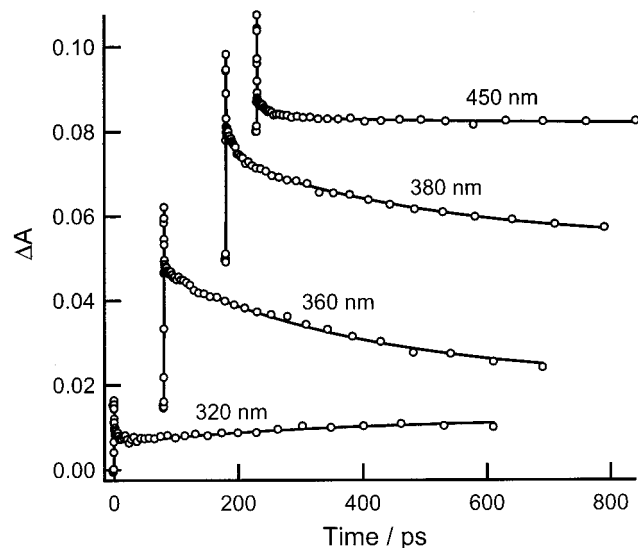


**Figure 2.** Single wavelength transients recorded at the indicated probe wavelengths following 266 nm photolysis of diphenyldiazomethane in acetonitrile. The solid curves are global nonlinear least-squares fits to the experimental points, shown as open circles. The fitting parameters are summarized in Table 1.

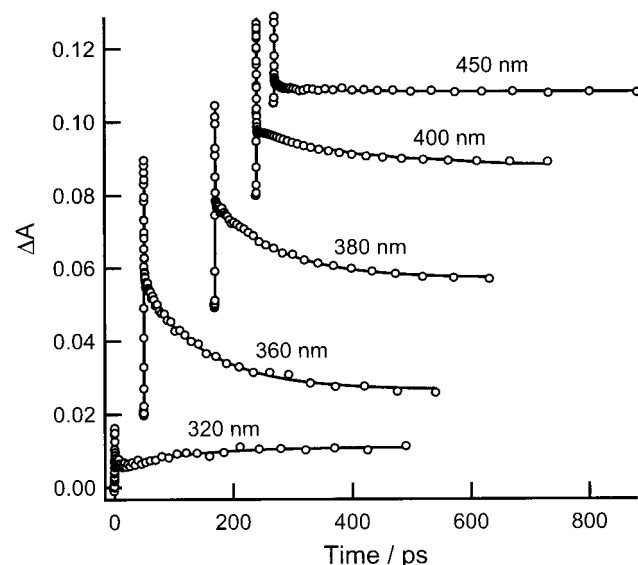


**Figure 3.** Same as Figure 2 for diphenyldiazomethane in cyclohexane.

diazomethane, as it was not observed in control experiments on solvent blanks. Following the spike, the signal evolves on a much slower time scale. Decays are observed for probe wavelengths  $\geq 360$  nm, while a rising signal is observed at 320 nm in both solvents. Transients in each solvent were globally fit at the probe wavelengths listed in Table 1 to the sum of three exponentials and a constant offset analytically convoluted with a Gaussian to model the instrument response function.<sup>14</sup> The fits are shown by the solid curves in Figures 2 and 3, and the best-fit values of the parameters are given in Table 1 for each solvent.

We assign the longest time constant ( $\tau_3$  in Table 1) to intersystem crossing (ISC) from  $^1\text{Ph}_2\text{C}$  to  $^3\text{Ph}_2\text{C}$ . The nearly 3-fold longer time constant in acetonitrile compared to cyclohexane is due to the pronounced effect of solvent polarity on

**Table 1.** Global Fit Parameters<sup>a</sup> for Transients in Figures 2 and 3

solvent	$\tau_1/\text{fs}$	$\tau_2/\text{ps}$	$\tau_3/\text{ps}$	$\lambda/\text{nm}$	$A_1$	$A_2$	$A_3$	$A_4$
$\text{CH}_3\text{CN}$	$270 \pm 40$	$21 \pm 2$	$340 \pm 20$	320	0.42	0.08	-0.16	0.34
				360	0.48	0.04	0.40	0.09
				380	0.58	0.09	0.27	0.05
				450	0.88	0.08	0.00	0.04
$\text{C}_6\text{H}_{12}$	$280 \pm 40$	$9 \pm 1$	$110 \pm 10$	320	0.49	0.06	-0.16	0.28
				360	0.64	0.05	0.25	0.06
				380	0.68	0.00	0.23	0.08
				400	0.76	-0.02	0.12	0.11
				450	0.86	0.03	0.03	0.07

<sup>a</sup> The model function was  $\Delta A = A_1 \exp(-t/\tau_1) + A_2 \exp(-t/\tau_2) + A_3 \exp(-t/\tau_3) + A_4$ . The amplitudes have been scaled such that  $\sum_i |A_i| = 1$ . The time constants,  $\tau_i$ , were global parameters in each solvent.

intersystem crossing.<sup>15</sup> Using a laser-induced fluorescence technique Eisenthal and co-workers reported an intersystem crossing rate of  $(110 \pm 12 \text{ ps})^{-1}$  in 3-methylpentane, a highly nonpolar solvent like cyclohexane.<sup>16,17</sup> In acetonitrile, they measured an intersystem crossing rate of  $(311 \pm 22 \text{ ps})^{-1}$ .<sup>16,18</sup> The excellent agreement with the decay times from our fits indicates that the absorption band with  $\lambda_{\text{max}} = 370$  nm is due to  $^1\text{Ph}_2\text{C}$ . Chergui and co-workers studied  $\text{Ph}_2\text{CN}_2$  by the femtosecond pump-probe technique.<sup>19</sup> Their pump wavelength was the same as in our study, but probing was done at just two wavelengths: 390 and 780 nm. They reported a time constant of  $\approx 100$  ps in isoctane in good agreement with our result in cyclohexane.

The rising signals at 320 nm are assigned to the growth of  $^3\text{Ph}_2\text{C}$  by ISC from  $^1\text{Ph}_2\text{C}$ . Absorption by  $^3\text{Ph}_2\text{C}$  was reported previously in single crystals,<sup>20</sup> in low-temperature glasses,<sup>21</sup> and in solution.<sup>22</sup> Hadel et al. reported  $\lambda_{\text{max}} = 314$  nm for  $^3\text{Ph}_2\text{C}$  in cyclohexane at room temperature.<sup>22</sup> The signal at 320 nm does not begin from the baseline after the completion of the subpicosecond dynamics observed near  $t = 0$ . Since very little ISC is expected just a few picoseconds after excitation of the diazo precursor, this suggests that  $^1\text{Ph}_2\text{C}$  has considerable absorption at 320 nm. The offsets at 320 nm are larger than at any other probe wavelength, consistent with the long lifetime of  $^3\text{Ph}_2\text{C}$ .

**(2) Singlet Diphenylcarbene Reactivity in Methanol.** The kinetics of the O-H insertion reaction of  $^1\text{Ph}_2\text{C}$  was studied in several neat alcohols. Figure 4 shows the transient spectra recorded at four different delay times after photoexcitation of  $\text{Ph}_2\text{CN}_2$  in methanol. The broad and intense spectrum observed 150 fs after the excitation pulse (Figure 4, squares) decays on a subpicosecond time scale as shown by the spectrum at 800 fs (Figure 4, crosses). A new absorption band with  $\lambda_{\text{max}} \approx 440$  nm appears next (Figure 4, filled circles). This band attains maximum amplitude 18 ps after the pump pulse and then decays toward the baseline. By 100 ps after the pump pulse there is

(15) Langan, J. G.; Sitzmann, E. V.; Eisenthal, K. B. *Chem. Phys. Lett.* **1984**, *110*, 521.

(16) The time constant is the reciprocal rate constant reported by Eisenthal and co-workers. The uncertainty in the time constant was computed by error propagation from the reported uncertainty in the rate.

(17) Dupuy, C.; Korenowski, G. M.; McAuliffe, M.; Hetherington, W. M. I.; Eisenthal, K. B. *Chem. Phys. Lett.* **1981**, *77*, 272.

(18) Eisenthal, K. B.; Turro, N. J.; Sitzmann, E. V.; Gould, I. R.; Hefferon, G.; Langan, J.; Cha, Y. *Tetrahedron* **1985**, *41*, 1543.

(19) Portella-Oberli, M. T.; Jeannin, C.; Soep, B.; Zerza, G.; Chergui, M. *Chem. Phys. Lett.* **1998**, *296*, 323.

(20) Closs, G.; Hutchison, C. A. J.; Kohler, B. E. *J. Chem. Phys.* **1966**, *44*, 413.

(21) Trozzolo, A. M.; Gibbons, W. A. *J. Am. Chem. Soc.* **1967**, *89*, 239.

(22) Hadel, L. M.; Platz, M. S.; Scavano, J. C. *J. Am. Chem. Soc.* **1984**, *106*, 283.

(14) A detailed description of our global fitting procedure can be found in ref 12.

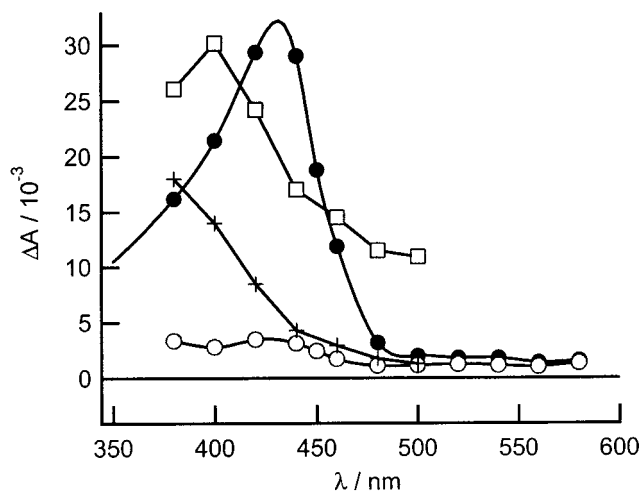


**Figure 4.** Transient spectra for diphenyldiazomethane in methanol 150 fs (squares), 800 fs (crosses), 15 ps (filled circles), and 100 ps (open circles) after the 266 nm pump pulse.

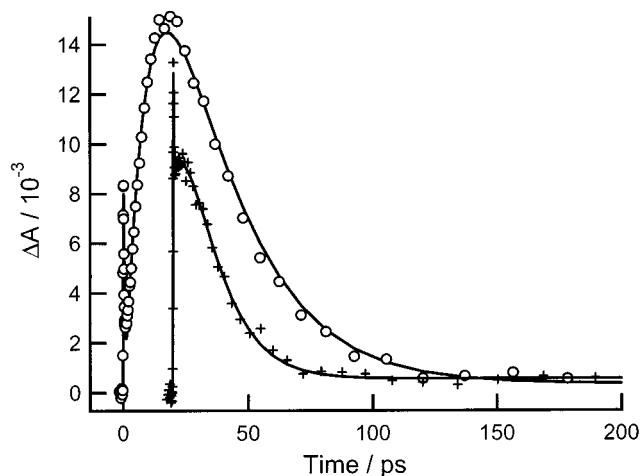


**Figure 5.** Transient absorption at 435 nm (circles) and at 360 nm (crosses) in  $\text{CH}_3\text{OH}$ . The 360 nm transient has been offset by 20 ps for clarity.

minimal transient absorption at  $\lambda \geq 370$  nm (open circles in Figure 4).

The asymmetric spectrum with  $\lambda_{\text{max}} \approx 435$  nm matches the well-known spectrum of diphenylmethyl cation ( $\text{Ph}_2\text{CH}^+$ ). Absorption by this carbocation was characterized in superacid conditions in the 1950s.<sup>23</sup> It was later detected transiently in pulse radiolysis<sup>24</sup> and pulsed laser experiments.<sup>25–27</sup> The dramatic growth and decay of  $\text{Ph}_2\text{CH}^+$  can be seen clearly in the single-wavelength scan recorded at 435 nm (circles in Figure 5). The signal rises to a maximum near  $t = 18$  ps before decaying back toward the baseline. Figure 5 also shows the decay of  $^1\text{Ph}_2\text{C}$  at 360 nm. A small rise with a maximum near 5 ps delay is due to absorption by  $\text{Ph}_2\text{CH}^+$  at this wavelength (see below).

**Deuterium Isotope Effect in Methanol.** The effect of isotopic substitution was studied in normal methanol ( $\text{CH}_3\text{OH}$ ) and O-deuterated methanol ( $\text{CH}_3\text{OD}$ ). Signals at 435 nm in these

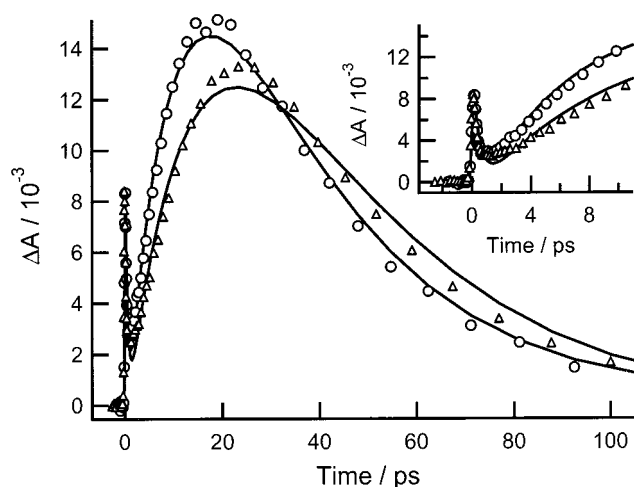


**Figure 6.** Transient absorption at 435 nm in  $\text{CH}_3\text{OH}$  (circles) and  $\text{CH}_3\text{OD}$  (triangles). The inset shows the early-time signals.

two solvents are compared in Figure 6. The data were recorded in back-to-back scans on solutions of  $\text{Ph}_2\text{CN}_2$  in  $\text{CH}_3\text{OH}$  and  $\text{CH}_3\text{OD}$ . Solutions with equal concentrations of the diazo precursor gave equal absorbance at the pump wavelength, making the relative signal magnitudes in Figure 6 significant. Within our experimental uncertainty, the spikelike signals at early time have the same amplitude and identical decay times in both solvents. At longer times, the two transients in Figure 6 have similar decay rates, but as the inset to Figure 6 shows, the rise times are different in the two solvents. Additionally, the signal in  $\text{CH}_3\text{OD}$  at 435 nm reaches a maximum at a later time than in  $\text{CH}_3\text{OH}$ . Rate constants determined by least-squares fitting (see below) confirm that the slower rate constant is the same in both solvents, while the faster step shows a kinetic isotope effect of  $k_{\text{H}}/k_{\text{D}} = 1.7$ .

### (3) Singlet Diphenylcarbene Reactivity in Other Alcohols.

Femtosecond pump–probe experiments were also carried out for  $\text{Ph}_2\text{CN}_2$  in a series of neat alcohols. Transients recorded at 435 nm are shown in Figure 7. This wavelength is the approximate maximum of the  $\text{Ph}_2\text{CH}^+$  absorption band in each of the alcohols investigated. The transients in Figure 7 were normalized such that the subpicosecond decays after  $t = 0$  have identical amplitude.

**(4) Dynamics in Tetrahydrofuran.** No evidence of an intermediate was seen when  $\text{Ph}_2\text{CN}_2$  was photolyzed in tetrahydrofuran. The transient absorption at 420 nm is shown in Figure 8. As in the other solvents, a pronounced, subpicosecond decay is observed. This is followed by a steadily decaying signal. By fitting a straight line to the logarithm of the signal at delay times  $t \geq 4$  ps, a decay constant of  $151 \pm 16$  ps was estimated.

**(5) Transient Absorption Actinometry.** Comparative actinometric measurements were performed to quantify the importance of protonation as a decay channel for  $^1\text{Ph}_2\text{C}$ . In these experiments, transient absorption signals from solutions of diphenyldiazomethane were compared with signals recorded under identical experimental conditions from a reference solution containing benzophenone (BP) in acetonitrile. The concentration of BP was adjusted to give the same ground-state absorbance at the pump wavelength of 266 nm as a second solution of diphenyldiazomethane in methanol. Under these conditions, and in the absence of multiphoton absorption and optical saturation, both solutions absorb the same number of photons, and quantum

(23) Deno, N. C.; Jaruzelski, J. J.; Schriesheim, A. *J. Am. Chem. Soc.* **1955**, *77*, 3044.

(24) Wang, Y.; Tria, J. J.; Dorfman, L. M. *J. Phys. Chem.* **1979**, *83*, 1946.

(25) Bartl, J.; Steenken, S.; Mayr, H.; McClelland, R. A. *J. Am. Chem. Soc.* **1990**, *112*, 6918.

(26) Bartl, J.; Steenken, S.; Mayr, H. *J. Am. Chem. Soc.* **1991**, *113*, 7710.

(27) Faria, J. L.; Steenken, S. *J. Phys. Chem.* **1993**, *97*, 1924.



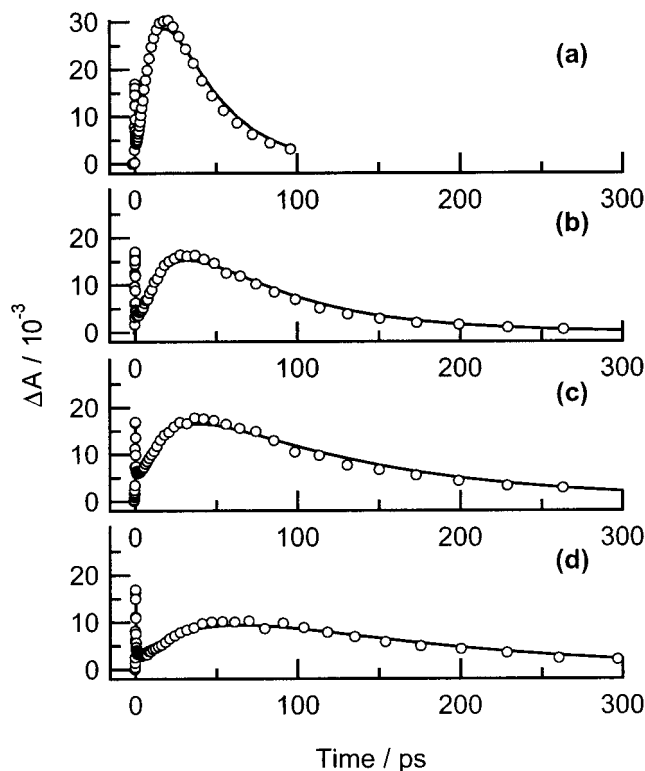


**Figure 7.** Transient absorption at 435 nm following 266 nm photolysis of diphenyldiazomethane in (a) methanol, (b) ethanol, (c) 1-propanol, and (d) 2-propanol.

yields and extinction coefficients can be estimated using the relation

$$\epsilon_X(\lambda) \phi_X(t) = \epsilon_{BP}(\lambda') \phi_{BP}(t') \frac{\Delta A_X(t, \lambda)}{\Delta A_{BP}(t', \lambda')} \quad (1)$$

In this equation,  $\epsilon$  denotes (molar decadic) absorption coefficients,  $\phi$  represents time-dependent quantum yields that account for population kinetics, and  $\Delta A(t, \lambda)$  is the transient absorption signal at probe wavelength  $\lambda$ , measured at time  $t$ . The subscripts X and BP label the solution under study ( $\text{Ph}_2\text{CN}_2$  in methanol) and the benzophenone/acetonitrile reference solution, respectively.

If more than one species contributes to the signal, then the product  $\epsilon\phi$  must be replaced by a sum over all absorbing species. As the time arguments in eq 1 indicate, signals from the reference system and system X can be compared at different delay times, and it is not necessary to measure the signals at the same probe wavelength, as long as the relative spectral amplitudes are accurate at the two wavelengths. This is achieved by making the spot size of the probe pulse at the sample several times smaller than the pump spot. The spectral fidelity of our transient absorption spectrometer has been demonstrated previously using the well-characterized spectrum of one-electron reduced methyl viologen.<sup>12</sup> Although this technique has been frequently employed in the past on slower time scales,<sup>28–31</sup> we believe this is the first application of the comparative method to femtosecond transient absorption experiments.

(28) Lutz, H.; Breheret, E.; Lindqvist, L. *J. Phys. Chem.* **1973**, *77*, 1758.

(29) Amand, B.; Bensasson, R. *Chem. Phys. Lett.* **1975**, *34*, 44.

(30) Wintgens, V.; Johnston, L. J.; Scaiano, J. C. *J. Am. Chem. Soc.* **1988**, *110*, 511.

(31) Bakac, A.; Burrows, H. D. *Appl. Spectrosc.* **1997**, *51*, 1916.

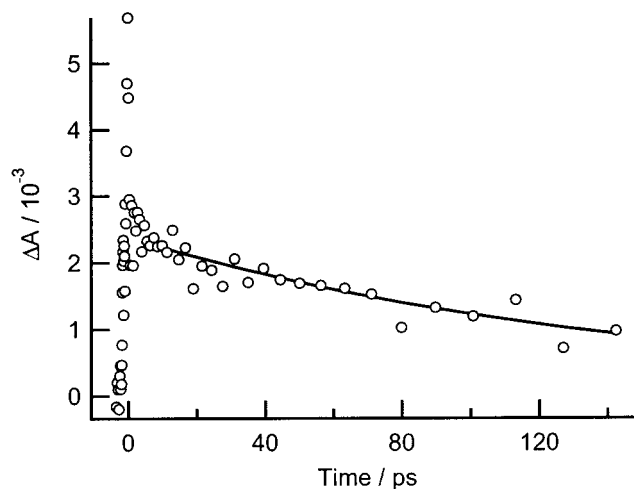


**Figure 8.** Transient absorption of  $\text{Ph}_2\text{CN}_2$  in tetrahydrofuran induced at a probe wavelength of 420 nm by a pump pulse at 266 nm. The solid line is the result of a linear least-squares fit to the logarithm of the long time data. The time constant obtained is  $151 \pm 16$  ps.

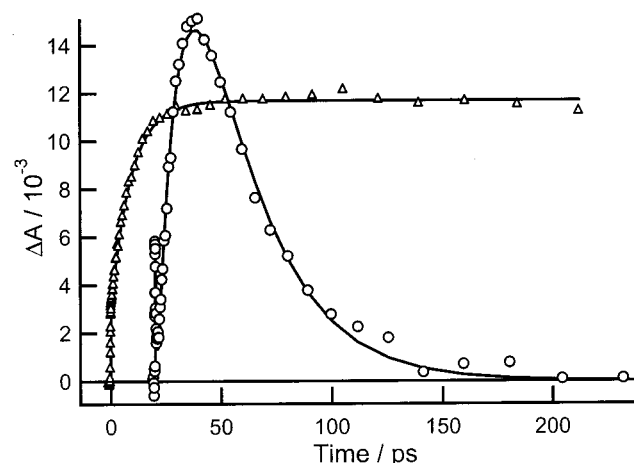


**Figure 9.** Signal comparison of equal absorbance solutions of benzophenone in acetonitrile (triangles) and diphenyldiazomethane in methanol (open circles). The latter curve is displaced by 20 ps for clarity. The probe wavelengths are 525 and 435 nm for benzophenone and diphenyldiazomethane, respectively.

The signal from benzophenone was recorded at 525 nm at the peak of its long-wavelength triplet–triplet absorption band. The signal, which is shown in Figure 9, rises with a single-exponential lifetime of  $9.2 \pm 1.2$  ps to a constant plateau. The rise time is in excellent agreement with the value  $9.6 \pm 0.9$  ps determined previously by femtosecond transient grating spectroscopy in acetonitrile.<sup>32</sup> This time constant reflects ultrafast ISC from the optically prepared singlet state. Following the completion of the rise, a constant transient absorption signal is observed over the entire delay range of our instrument (0–1000 ps), consistent with the long-lived BP triplet state ( $\tau \approx 14 \mu\text{s}$  in acetonitrile<sup>33</sup>).

The ratio of the maximum signal in methanol at 435 nm to the BP triplet at 50 ps is 1.25 from the data in Figure 9. The molar absorption coefficient of the benzophenone triplet state is  $\epsilon_{BP}(525\text{nm}) = 6500 \text{ M}^{-1} \text{ cm}^{-1}$ , and the triplet quantum yield,  $\phi_{BP}$ , is equal to unity.<sup>33</sup> The molar absorption coefficient of

(32) Tamai, N.; Asahi, T.; Masuhara, H. *Chem. Phys. Lett.* **1992**, *198*, 413.

(33) Gramain, J.-C.; Remuson, R. *J. Chem. Soc., Faraday Trans. 1* **1980**, *76*, 1800.

$\text{Ph}_2\text{CH}^+$  has not been reported in neat methanol due to the cation's short lifetime in this nucleophilic solvent. To estimate this quantity, we used the value measured in acetonitrile,  $\epsilon(435\text{nm}) = 44\,000\text{ M}^{-1}\text{ cm}^{-1}$ .<sup>25</sup> Little is known about solvent effects on  $\text{Ph}_2\text{CH}^+$  absorption; however, similar absorption is expected in methanol and acetonitrile on account of their similar dielectric properties. Using these values in eq 1,  $\phi = 0.18$  is calculated for  $\text{Ph}_2\text{CH}^+$  at 18 ps, the time of its maximum concentration. The uncertainty in the quantum yield is estimated to be 20–30%.<sup>34</sup>

## Discussion

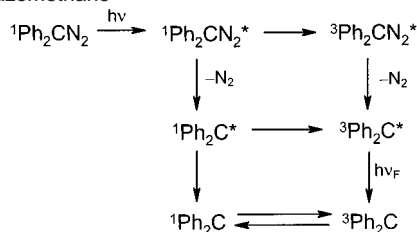
**(1) Formation of Singlet Diphenylcarbene from Diphenyldiazomethane.** The absorption spectrum of  $^1\text{Ph}_2\text{C}$  has not been reported previously. Dix and Goodman studied two diphenylcarbene derivatives, bis(*p*-chlorophenyl)carbene and bis(*p*-methoxyphenyl)carbene, using 355 nm laser flash photolysis with 25 ps pulses.<sup>4</sup> They observed transient absorption between 400 and 500 nm in heptane, tetrahydrofuran, and acetonitrile, which they assigned to the singlet carbenes. They failed to detect transient absorption between 400 and 700 nm upon picosecond photolysis of  $\text{Ph}_2\text{CN}_2$ . The absorption spectrum of  $^1\text{Ph}_2\text{C}$  (Figure 1) is blue-shifted relative to the spectra reported by Dix and Goodman. The same spectral blue shift is observed when the absorption spectrum of  $\text{Ph}_2\text{CH}^+$  is compared to those of the para-substituted cations.<sup>25</sup> Turro et al. reported  $\lambda_{\text{max}} = 355\text{ nm}$  for the singlet state of phenylchlorocarbene.<sup>35</sup> Absorption near 360 nm appears to be a general characteristic of singlet aryl carbenes. Ab initio calculations indicate that these transitions have considerable  $\pi-\pi^*$  character and involve molecular orbitals that are delocalized over the phenyl rings.<sup>36</sup>

As seen in Figure 1,  $\lambda_{\text{max}}$  of  $^1\text{Ph}_2\text{C}$  has approximately the same value in highly polar acetonitrile as in nonpolar cyclohexane. In contrast, the absorption spectrum of the lowest singlet state of 2-naphthyl(carbomethoxy)carbene depends significantly on the solvent.<sup>36</sup> Ab initio calculations combined with a realistic solvation model have reproduced both effects.<sup>36</sup>

The intermediate time constant ( $\tau_2$  in Table 1) has the smallest amplitude at each probe wavelength. We assign this weak signal component to vibrational cooling of the nascent  $^1\text{Ph}_2\text{C}$ . Eisenthal and co-workers observed  $^3\text{Ph}_2\text{C}^*$  fluorescence following single photon excitation of  $\text{Ph}_2\text{CN}_2$  at 266 nm from which they concluded that the carbon–nitrogen bond strength is  $<2\text{ eV}$ .<sup>17</sup> A high-level ab initio estimate of the minimum carbon–nitrogen bond dissociation energy for gas-phase  $\text{CH}_2\text{N}_2$  with respect to singlet products gave a value  $D_e = 38.2\text{ kcal mol}^{-1}$  (1.7 eV).<sup>37</sup> Simon and Peters reported a value  $\Delta_r H = 0.0 \pm 1.7\text{ kcal mol}^{-1}$  for the dissociation of  $\text{Ph}_2\text{CN}_2$  to  $^3\text{Ph}_2\text{C}$  and molecular nitrogen in benzene.<sup>38</sup> Even though this value is a lower limit, it provides evidence that the carbon–nitrogen bond of diazo compounds is indeed weak.

Following photolysis of the weak carbon–nitrogen bond, the  $^1\text{Ph}_2\text{C}$  fragment is expected to have at least 2.6 eV (21 000  $\text{cm}^{-1}$ )

**Scheme 2.** Deactivation Pathways for Photoexcited Diphenyldiazomethane



of excess vibrational energy. Vibrationally hot molecules display red-shifted absorption spectra that blue shift as they thermally equilibrate with the cooler solvent molecules.<sup>39,40</sup> Transient absorption at probe wavelengths on the red edge of a given absorption band generally show decays, while signals at higher energy show rises. The decay times observed here (9 ps in cyclohexane and 21 ps in acetonitrile) are in line with times observed for other polyatomic molecules. For example, Troe's group reported deactivation times of  $\approx 14\text{ ps}$  for azulene in cyclohexane and acetonitrile.<sup>41</sup> Since vibrational cooling usually results in probe wavelength dependent decay times, the characterization of this process by a single, global fitting parameter is approximate. We previously reported evidence for vibrational cooling in 2-naphthyl(carbomethoxy)carbene following UV photolysis of its diazo precursor.<sup>8</sup>

The subpicosecond decay observed immediately after excitation of  $\text{Ph}_2\text{CN}_2$  is the most enigmatic feature of the dynamics. This spikelike signal was seen in all solvents investigated, and in our earlier study of 2-naphthyl(carbomethoxy)carbene.<sup>8</sup> Since the signal at all times changes linearly with pump pulse energy, multiphoton excitation is not responsible. Chergui and co-workers observed a  $\approx 250\text{ fs}$  decay following UV photolysis of  $\text{Ph}_2\text{CN}_2$  in isoctane at 390 and 780 nm.<sup>19</sup> They assigned this dynamical feature to energy relaxation in the hot carbene by internal conversion and vibrational relaxation. The spectrum during this phase of the signal (squares in Figure 4) resembles a broadened version of the  $^1\text{Ph}_2\text{C}$  spectrum shown in Figure 1, as expected for a vibrationally hot species.<sup>42</sup> However, vibrational cooling in the lowest singlet state of  $^1\text{Ph}_2\text{C}$  was excluded for two reasons. First, vibrational cooling of hot molecules typically occurs on a time scale of order 10 ps.<sup>42</sup> Second, pronounced decays are observed at 320 and 360 nm on the high-energy side of the  $^1\text{Ph}_2\text{C}$  absorption band. In contrast, rising signals are usually observed at probe wavelengths on the blue edge of the absorption band of vibrationally hot molecules.<sup>40</sup>

The short-time dynamics are difficult to assign because so little is known about the earliest events following electronic excitation of diazo compounds. Scheme 2 shows some possible deactivation pathways. The initially prepared excited singlet state of the diazo ( $^1\text{Ph}_2\text{CN}_2^*$ ) could intersystem cross to a triplet diazo state, lose nitrogen, or internally convert to regenerate the ground-state diazo compound. Since we have ruled out absorption by  $^1\text{Ph}_2\text{C}$  or  $^3\text{Ph}_2\text{C}$  for the short-time signal, absorption by an excited state must be considered. Excited-state absorption by  $^3\text{Ph}_2\text{C}^*$  is unlikely given the nanosecond lifetime of this state.<sup>43,44</sup> As already mentioned, Eisenthal and co-workers

(34) Previous measurements of  $\epsilon$  for  $\text{Ph}_2\text{CH}^+$  in various solvents are summarized in ref 25. On the basis of these values, a cautious estimate of the uncertainty in the molar absorption coefficient of  $\text{Ph}_2\text{CH}^+$  is 20–30%. The uncertainty in the quantum yield will be roughly the same, since the other quantities required for the calculation are known more precisely.

(35) Turro, N. J.; Butcher, J. A., Jr.; Moss, R. A.; Guo, W.; Munjal, R. C.; Fedorynski, M. *J. Am. Chem. Soc.* **1980**, *102*, 7576.

(36) Peon, J.; Kohler, B.; Barone, V.; Hadad, C. M.; Platz, M. S. To be submitted for publication.

(37) Papakondylis, A.; Mavridis, A. *J. Phys. Chem. A* **1999**, *103*, 1255.

(38) Simon, J. D.; Peters, K. S. *J. Am. Chem. Soc.* **1988**, *110*, 3336.

(39) Laerner, F.; Elsaesser, T.; Kaiser, W. *Chem. Phys. Lett.* **1989**, *156*, 381.

(40) Miyasaka, H.; Hagihara, M.; Okada, T.; Mataga, N. *Chem. Phys. Lett.* **1992**, *188*, 259.

(41) Schwarzer, D.; Troe, J.; Votsmeier, M.; Zerezke, M. *J. Chem. Phys.* **1996**, *105*, 3121.

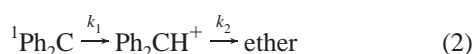
(42) Elsaesser, T.; Kaiser, W. *Annu. Rev. Phys. Chem.* **1991**, *42*, 83.

detected a small amount of the triplet–triplet fluorescence at 510 nm from  $^3\text{Ph}_2\text{C}^*$ , which appeared within their instrumental resolution.<sup>17,43</sup> Since this excited triplet population has a singlet-state precursor, it is possible that some or all of the  $^1\text{Ph}_2\text{C}$  is formed in an electronically excited state,  $^1\text{Ph}_2\text{C}^*$ . This population would then internally convert to  $^1\text{Ph}_2\text{C}$  in competition with intersystem crossing to  $^3\text{Ph}_2\text{C}^*$ . Internal conversion between upper singlet states is thought to occur in hundreds of femtoseconds, consistent with the fast decay of the short-time signal. However, the strength of the transition necessary to explain the spikelike feature seems inconsistent with the generally weak absorption of upper singlet states.

In our opinion, the most likely possibility for the short-time signal is absorption by the initial diazo excited state,  $^1\text{Ph}_2\text{CN}_2^*$ . In this case, the ultrafast decay rate is the sum of the rates of all deactivation processes, including  $\text{N}_2$  extrusion, intersystem crossing, and internal conversion to the diazo ground state. The decay time of  $\approx 300$  fs indicates that carbon–nitrogen bond scission is not impulsive, suggesting that the excited-state potential is not purely repulsive. The strong wavelength dependence of the photodestruction quantum yields of diazo compounds<sup>45</sup> is consistent with excited-state deactivation pathways other than  $\text{N}_2$  loss. In addition, the broad absorption band of the short-time feature, which extends from 320 to beyond 500 nm (squares in Figure 4), resembles the spectrum of  $\text{Ph}_2\text{CN}_2^{*-}$  reported by Chateaufeuf.<sup>46,47</sup> Excited-state absorption by singlet states of aromatic compounds frequently resembles that of the corresponding radical anions due to their similar electronic configurations.

There are few reports of photophysical measurements for diazo compounds. Kirmse determined a quantum yield of photodestruction of 0.78 for diphenyldiazomethane exposed to quasi-monochromatic light at 294 nm.<sup>45</sup> Quantum yields were approximately 10-fold smaller when the diazo compound was excited in its long wavelength absorption band.<sup>45</sup> The quantum yields for other diazo compounds were significantly lower. This suggests that other pathways must compete with  $\text{N}_2$  extrusion in the singlet excited state of  $\text{Ph}_2\text{CN}_2$ . Silva and Thomas reported a quantum yield of photolysis of  $\approx 0.05$  for 1-pyrenyldiazomethane for excitation between 340 and 380 nm.<sup>48</sup> They observed both fluorescence and ISC in this compound, which they attributed to strong mixing between electronic states of pyrene with those of the diazo group. Clearly, an important question to answer in the future is the quantum yield of  $\text{N}_2$  loss and the primary quantum yield for  $^1\text{Ph}_2\text{C}$  formation.

**(2)  $\text{Ph}_2\text{CH}^+$  Growth and Decay. (a) Sequential First-Order Reaction Kinetics.** The pronounced rise and decay of the transient absorption signals in Figure 6 offer a striking example on the ultrafast time scale of the time-dependent population of an intermediate in a sequential two-step reaction mechanism:



In eq 2, the rate of proton transfer is given by  $k_1$ , while solvolysis of the diphenylmethyl cation occurs with rate  $k_2$ . We treat both

steps by first-order kinetics, even though the decay of the carbenium ion could exhibit more complex, nonclassical kinetics due to reaction in the geminate ion pair (pathway A' in Scheme 1). This issue is discussed in more detail later. We define  $C(t)$  to be the ratio of the  $\text{Ph}_2\text{CH}^+$  population to the initial population of  $^1\text{Ph}_2\text{C}$ . Since no  $\text{Ph}_2\text{CH}^+$  is present at time zero,  $C(t)$  is given by

$$C(t) = \frac{k_1}{k_1 - k_2} [\exp(-k_2 t) - \exp(-k_1 t)] \quad (3)$$

The maximum value of  $C(t)$ ,  $C_{\text{max}}$ , depends only on the ratio,  $r = k_1/k_2$ , of the two rate constants:

$$C_{\text{max}} = r^{1/(1-r)} \quad (4)$$

For small  $r$  (i.e.  $k_1 \ll k_2$ ), there is negligible intermediate population at all times ( $C_{\text{max}} \approx 0$ ), while for large  $r$ , population accumulates in the intermediate state, before decaying to product ( $C_{\text{max}} \approx 1$ ). Of course, regardless of the value of  $r$ , every  $^1\text{Ph}_2\text{C}$  is eventually protonated, according to eq 2. Equation 4 quantifies the maximum amount of intermediate that can be detected at one instant. This quantity is measured in our experiments (see Figure 9) and will be discussed in more detail later.

Fitting transient signals from intermediates such as those in Figure 6 to eq 3 is difficult for two reasons. First, it is challenging to accurately determine values of  $k_1$  and  $k_2$  by nonlinear least-squares fitting. In the presence of noise, extracting rate constants from multiexponential decays can be highly uncertain, particularly when the rates do not differ significantly.<sup>49</sup> Second, even when the rates can be accurately determined by fitting, the association of rate constants with individual reaction steps can be ambiguous.<sup>50</sup> The decaying signal at long times is always due to the step with the lower rate, but the rate-limiting step can be either the first or second step in eq 2.<sup>51</sup> Our solutions to these difficulties are presented in the next two subsections.

**(b) Determination of  $k_1$  and  $k_2$ .** Attempts at fitting the signals to a biexponential function of the form  $A_1 e^{-k_1 t} + A_2 e^{-k_2 t}$  by nonlinear least squares generally did not produce unique values of the parameters.<sup>52</sup> To obtain reliable estimates, the natural logarithm of the signal at delay times  $t$  greater than a cutoff time,  $t_{\text{cut}}$ , was fit to a straight line. The slope of this line

(49) Istratov, A. A.; Vyvenco, O. F. *Rev. Sci. Instrum.* **1999**, *70*, 1233.

(50) Measurement of the rate of disappearance of  $^1\text{Ph}_2\text{C}$  (or the rate of formation of the ether) eliminates this ambiguity. Unfortunately, the UV-absorbing ether product is not detected in our experiments. The singlet absorption can be monitored as already shown in Figures 2 and 3. In methanol, however, transient absorption at this wavelength contains a significant contribution by  $\text{Ph}_2\text{CH}^+$  due to the strength of this transition. This results in the weak maximum seen at 360 nm in Figure 5. Due to the admixture of  $^1\text{Ph}_2\text{C}$  and  $\text{Ph}_2\text{CH}^+$  this signal's decay is governed by both rate constants, just like the signal at 435 nm, and assignment is not possible.

(51) The emission from pyrene excimers illustrates the kinetics of an intermediate in the limit  $k_2 > k_1$ . See: Van Dyke, D. A.; Pryor, B. A.; Smith, P. G.; Topp, M. R. *J. Chem. Educ.* **1998**, *75*, 615. In this case, the growth of the time-resolved excimer emission is determined not by the time scale of their formation but by their short emission lifetime.

(52) This is a reflection of the flat nature of the  $\chi^2$  surface with respect to  $\tau_1$  and  $\tau_2$ . For example, the data from  $\text{Ph}_2\text{CH}^+$  in ethanol (Figure 8b) were fit by holding  $\tau_1$  constant but allowing the other parameters to be optimized. When  $\tau_1$  was varied between 20 and 34 ps for the fit varied by less than 12%. Although the fits all appeared very good by eye, closer inspection showed that many of them failed to accurately reproduce the long-time signal decay. Note that independent amplitudes must be used (as opposed to eq 3) since the signal at 435 nm contains contributions from both  $^1\text{Ph}_2\text{C}$  and  $\text{Ph}_2\text{CH}^+$ . Since  $\text{Ph}_2\text{CH}^+$  absorption dominates, the best-fit values of  $A_1$  and  $A_2$  are nearly equal and of opposite sign.

(43) Wang, Y.; Sitzmann, E. V.; Novak, F.; Dupuy, C.; Eisenthal, K. B. *J. Am. Chem. Soc.* **1982**, *104*, 3238.

(44) Horn, K. A.; Allison, B. D. *Chem. Phys. Lett.* **1985**, *116*, 114.

(45) Kirmse, W.; Horner, L. *Justus Liebigs Ann. Chem.* **1959**, 625, 34.

(46) Chateaufeuf, J. E. *J. Phys. Chem.* **1990**, *94*, 7177.

(47) Chateaufeuf, J. E. *Chem. Phys. Lett.* **1992**, *188*, 439.

(48) Silva, S.; Olea, A. F.; Thomas, J. K. *Photochem. Photobiol.* **1991**, *54*, 511.



**Table 2.** Time Constants<sup>a</sup> for Formation ( $\tau_1$ ) and Decay ( $\tau_2$ ) of Diphenylmethyl Cation in Neat Alcohols and Protonation Fractions ( $f_p$ )

solvent	$\tau_1$ /ps	$\tau_2$ /ps	$\tau_{\text{sol}}^b$ /ps	$C_{\text{max}}^c$	$\Delta A_{\text{max}}/\Delta A_{\text{max}}^{\text{CH}_3\text{OH}}$	$f_p^d$
CH <sub>3</sub> OH	9.0 ± 0.5	30.5 ± 1.5	5.0, <sup>e</sup> 6.80 ± 0.05 <sup>f</sup>	0.60	1	0.30
CH <sub>3</sub> OD	15 ± 1	34.8 ± 2.1	7.46 ± 0.05 <sup>f</sup>	0.53	0.88	0.30
ethanol	16 ± 2	65 ± 6	16 <sup>e</sup>	0.63	0.54	0.15
1-propanol	17 ± 2	117 ± 8	26 <sup>e</sup>	0.72	0.54	0.14
2-propanol	35 ± 5	130 ± 15		0.62	0.31	0.09

<sup>a</sup> See text for detailed description of fitting procedure. Uncertainties are estimated standard deviations from the fits, assuming a standard deviation of  $3 \times 10^{-4}$  for an individual  $\Delta A$  measurement. <sup>b</sup> Solvation times determined by dynamic Stokes shift measurements. <sup>c</sup> Evaluated from eq 4 and  $r = \tau_2/\tau_1$ . <sup>d</sup> Protonation fraction, see text for details. <sup>e</sup> From ref 76. <sup>f</sup> From ref 62.

fixed the value of the slower rate constant, which was labeled  $k_2$ . It will be shown in the next section that  $k_2$  actually is the rate constant for the second reaction step in eq 2. Use of the long-time signal decay to determine the slowest rate constant of a multiexponential function is known as the peeling method.<sup>49</sup> An initial guess for the value of  $t_{\text{cut}}$  was made by eye from a log plot of the signal. It was verified in every case that  $t_{\text{cut}}$  was always 3–5 times greater than  $\tau_1 = 1/k_1$ . Next, nonlinear least-squares fitting was used to determine the value of  $k_1$ , holding  $k_2$  fixed at the value determined in the first step. The value of  $k_2$  was insensitive to the precise value of  $t_{\text{cut}}$ . The time constants,  $\tau_{1,2} = 1/k_{1,2}$ , determined by this procedure are listed in Table 2. The fits are shown by the solid curves in Figures 5–7.

Chateaneuf studied Ph<sub>2</sub>CN<sub>2</sub> photolysis on the picosecond time scale in several alcohols.<sup>3</sup> In his experiments, Ph<sub>2</sub>CH<sup>+</sup> was formed within the duration of the 18 ps, 355 nm pump pulse used to photoexcite diphenyldiazomethane. The cation population decayed in 40, 70, and 85 ps in methanol, ethanol, and 2-propanol, respectively. There is good agreement with our  $\tau_2$  values in methanol and ethanol. However, the decay time of Ph<sub>2</sub>CH<sup>+</sup> reported here in 2-propanol ( $\tau = 130$  ps) is considerably slower than the value reported by Chateaneuf. The reason for this discrepancy is unclear at present. There are no previous direct measurements of  $\tau_1$  to compare our values with. It will be shown later that the  $\tau_1$  values are consistent with rate constants inferred from product studies for the reaction of <sup>1</sup>Ph<sub>2</sub>C with alcohols.

**(c) Protonation More Rapid Than Solvolysis.** As already noted, fitting to the intermediate's growth and decay does not by itself determine whether the first or second step of eq 2 has the faster rate. Decisive evidence that protonation is the faster step comes from the solvent isotope effect in methanol. The fitting results in Table 2 indicate that the fast step has an isotope effect, while the slower step shows a much smaller change of only 14%, which is close to our experimental uncertainty. An isotope effect is expected for protonation of singlet diphenylcarbene (pathway A in Scheme 1). On the other hand, the disappearance of Ph<sub>2</sub>CH<sup>+</sup> due to reaction with either an alkoxide ion (pathway A') or a neutral alcohol molecule is not expected to show an isotope effect. Since  $\tau_1$  shows an isotope effect, we conclude that it is the time constant of protonation. If ylide formation were the correct mechanism (pathway B in Scheme 1), then an isotope effect would be expected for the second step (proton shift shown by pathway B'), but not for the first (electrophilic attack). In this case,  $\tau_1$  and  $\tau_2$  would be associated with the second and first steps of eq 2, respectively. While an argument can be made that an intramolecular proton shift should occur more rapidly than attack by a carbene electrophile on a neutral alcohol molecule, the results in the ether THF rule out ylide formation. In this solvent, which lacks an acidic proton,

there was no spectroscopic evidence of an ylide reaction intermediate. Additionally, the decay of <sup>1</sup>Ph<sub>2</sub>C was no faster than is expected for ISC in this solvent.<sup>15,53</sup>

Further evidence that  $\tau_1$  in Table 2 is the time constant for proton transfer is provided by the relative signal amplitudes in CH<sub>3</sub>OH and CH<sub>3</sub>OD at 435 nm. From the data in Figure 6, the ratio of the maximum signal in CH<sub>3</sub>OD to the maximum signal in CH<sub>3</sub>OH is 0.87. This ratio can be independently calculated from eq 4 and the measured time constants. Using the values of  $\tau_1$  and  $\tau_2$  in Table 2,  $C_{\text{max}}(\text{CH}_3\text{OD})/C_{\text{max}}(\text{CH}_3\text{OH}) = 0.88$ . On the other hand, interchanging the values of  $\tau_1$  and  $\tau_2$  yields a value of 1.3 for  $C_{\text{max}}(\text{CH}_3\text{OD})/C_{\text{max}}(\text{CH}_3\text{OH})$ . Thus, assignment of  $\tau_1$  to protonation is the only way to reproduce the observed isotope effect. A tacit assumption in this analysis is that the molar absorption coefficient of Ph<sub>2</sub>CH<sup>+</sup> in CH<sub>3</sub>OH is the same at 435 nm as that of Ph<sub>2</sub>CD<sup>+</sup> in CH<sub>3</sub>OD. We are unaware of any data on the effect of deuteration on carbocation absorption. The absorption spectrum of Ph<sub>2</sub>CH<sup>+</sup> is insensitive to solvent,<sup>26</sup> so a solvent isotope effect on the absorption spectrum can be ruled out. By the Born–Oppenheimer approximation, the potential energy surfaces of both cations are identical. A difference in absorption would require that one or more vibrational modes sensitive to deuteration be strongly coupled to the electronic transition. The compound 3-hydroxyflavone, which has an exchangeable proton, shows identical absorption in CH<sub>3</sub>OH and CH<sub>3</sub>OD.<sup>54</sup> Identical absorption by the two cations thus appears reasonable.

**(3) Decay Rates of <sup>1</sup>Ph<sub>2</sub>CH<sup>+</sup> in Neat Alcohols.** Protonation of diphenylcarbene by alcohol creates an alkoxide/Ph<sub>2</sub>CH<sup>+</sup> ion pair. This reaction is essentially irreversible due to the high basicity of the carbene. Thus, geminate *recombination* of the two partners to reform the alcohol and <sup>1</sup>Ph<sub>2</sub>C is not important. However, geminate *reaction* is possible in which Ph<sub>2</sub>CH<sup>+</sup> undergoes nucleophilic attack by the alkoxide ion to yield the ether product, as shown by pathway A' in Scheme 1. However, carbocations are highly electrophilic, and they react rapidly with any available nucleophile, including a solvent molecule.<sup>55</sup> Thus, the final ether product could also be formed by electrophilic addition of an alcohol molecule to the carbocation, giving rise to an oxonium ion, which subsequently deprotonates. On one hand, the Coulombic attraction of the two ions for each other could provide a strong driving force for ion pair collapse. On the other hand, the large number of neutral alcohol molecules surrounding the carbocation in the neat solvent might favor the homogeneous reaction. In this section, we discuss our current understanding of the importance of these two different channels for the different alcohols studied.

(53) This value was estimated from data in Figure 1 of ref 15.

(54) Strandjord, A. J. G.; Barbara, P. F. *J. Phys. Chem.* **1985**, *89*, 2355.

(55) McClelland, R. A. *Tetrahedron* **1996**, *52*, 6823.



In methanol and ethanol, the reaction of  $\text{Ph}_2\text{CH}^+$  with a neutral alcohol molecule appears to dominate ion pair collapse. Bartl et al. measured the rates of reaction between  $\text{Ph}_2\text{CH}^+$  and various nucleophilic quenchers, including neutral alcohol molecules, by nanosecond photolysis of  $\text{Ph}_2\text{CHCl}$  in acetonitrile.<sup>25,26</sup> From these rates and the molarities of the neat solvents, time constants of 34, 69, and 246 ps are predicted for methanol, ethanol, and 2-propanol, respectively. Our measured decay times in methanol and ethanol ( $\tau_2$  in Table 2) agree very well with these estimates, and we conclude that solvolysis by a neutral molecule is faster than addition of the geminate alkoxide ion to  $\text{Ph}_2\text{CH}^+$ . In the case of 2-propanol, however, the value of  $\tau_2$  in Table 2 is nearly a factor of 2 smaller than predicted from the bimolecular rate constant measured in acetonitrile by Bartl et al.

Of course, caution must be used when extrapolating bimolecular rate constants measured in acetonitrile to the neat alcohol solvents. Kirmse et al. reported pronounced solvent effects on the reaction rates of  $\text{Ph}_2\text{CH}^+$  with a given nucleophile.<sup>56</sup> These authors found that reaction rates were 40–100 times lower in 2,2,2-trifluoroethanol (TFE) than in acetonitrile, while still lower rates were observed in 3,3,3,3',3',3'-hexafluoro-2-propanol (HFIP). They argued that hydrogen bonding to the nucleophile hinders its reaction with the carbocation.<sup>56</sup> However, lower rates of reaction with increasing hydrogen bonding would predict slower rates in the neat solvents, in contrast to our observation in 2-propanol. In other systems, scavenging rates have been reported to increase faster than expected with quencher concentration. For example, a plot of the decay rate of  $\text{Ph}_2\text{CH}^+$  vs alcohol concentration shows upward curvature in 1,2-dichloroethane<sup>57</sup> and in HFIP.<sup>56</sup> Kirmse et al. rationalized this behavior by the ability of a second alcohol molecule to act as a base, preventing dissociation of an initial alcohol–carbocation adduct.<sup>56</sup> In this case, it is unclear why this mechanism would accelerate quenching in 2-propanol, but not in ethanol and methanol. In the latter two solvents the decay rates agree with those inferred from measurements of the bimolecular rate constants at low alcohol concentration. Furthermore, the quenching rates for alcohols in acetonitrile were reported to be independent of alcohol concentration.<sup>58</sup>

The anomalous kinetics in 2-propanol are best explained in our view by reaction between  $\text{Ph}_2\text{CH}^+$  and the alkoxide ion formed by protonation of the carbene. The reactive decay of this ion pair is apparently faster than nucleophilic attack by neutral 2-propanol, which is a weaker nucleophile than either methanol or ethanol. A crude estimate is that  $\text{Ph}_2\text{CH}^+$  and the 2-propoxide ion react in 100 ps. The geminate reaction rate is likely limited by the energetic cost of desolvating two singly charged ions in order for reaction to take place. If the rate of protonation of  $^1\text{Ph}_2\text{C}$  is controlled by the solvent reorganization necessary to solvate the incipient alkoxide ion (see next section), then solvent separated alkoxide/ $\text{Ph}_2\text{CH}^+$  ion pairs could be formed quickly.<sup>59</sup> The large reorganization energies associated

with solvent separated ion pairs are familiar from electron transfer in polar solvents.<sup>60</sup> This could retard the geminate reaction, offsetting the Coulombic attraction of the two oppositely charged ions. Further study is required to fully understand the competition between geminate ion pair collapse and reaction with a neutral alcohol molecule. A similar competition occurs in excited-state proton-transfer reactions to solvent at low pH. Complex kinetics can be observed in these systems due to the diffusion-influenced reaction of geminate partners. These effects can be modeled with the time-dependent Smoluchowski equation.<sup>61</sup>

To end this section, we note that the rate of decay of the diphenylmethyl cation is just 10% slower in  $\text{CH}_3\text{OD}$  than in  $\text{CH}_3\text{OH}$ . Yoshihara and co-workers determined by dynamic Stokes shift measurements that solvation of photoexcited coumarin 102 occurs approximately 10% more slowly in deuterated methanol.<sup>62</sup> This small isotope effect is thus consistent with rate-limiting solvation and is not believed to indicate proton transfer.

**(4) Intermolecular Proton Transfer from Alcohols to  $^1\text{Ph}_2\text{C}$ .** The  $\tau_1$  values in Table 2 show that proton transfer from oxygen to carbon can take place on an ultrafast time scale. Intermolecular proton transfer reactions are challenging to study by time-resolved methods because of the difficulty of initiating reaction at the same instant of time for an ensemble of donors and acceptors. Photoacids, molecules that undergo proton-transfer reactions in an electronically excited state, overcome this problem and have been extensively studied in recent years.<sup>63–65</sup> The fastest known photoacids transfer a proton to a water molecule in slightly less than 10 ps. Excited-state proton transfer to  $\text{H}_2\text{O}$  occurs in  $8 \pm 1$  ps at 25 °C for 5-cyano-1-naphthol<sup>63</sup> and in 7.1 ps for 7-hydroxy-4-methylflavylium.<sup>66</sup> Proton transfer from excited 8-hydroxypyrene-1,3,6-trisulfonate to acetate ion, which is present at high concentration in aqueous solution, occurs in 3 ps.<sup>64</sup>  $^1\text{Ph}_2\text{C}$ , which accepts a proton in 9 ps in neat methanol, belongs to this same class of ultrafast intermolecular proton-transfer reactions. Interestingly, proton transfer to methanol by 5-cyano-1-naphthol is nearly 2 orders of magnitude slower than in water, requiring 390 ps in  $\text{CH}_3\text{OH}$ .<sup>63</sup>

The high basicity of singlet carbenes follows from the high  $\text{p}K_{\text{a}}$  values of their corresponding carbocations. For example, the stable carbene imidazole-2-ylidene, which deprotonates weakly acidic hydrocarbons such as indene, is estimated to have a  $\text{p}K_{\text{a}}$  of 24, or a  $\text{p}K_{\text{b}}$  of  $-10$ .<sup>67</sup> By comparison, the powerful photoacid 5-cyano-1-naphthol has an excited-state  $\text{p}K_{\text{a}}$  of  $-2.8$ .<sup>63</sup> Ab initio calculations predict a lower proton affinity for imidazol-2-ylidene<sup>68</sup> than for diphenylcarbene,<sup>9</sup> suggesting that the latter may be even more basic.

The rate constant for the disappearance of singlet carbenes longer lived than  $^1\text{Ph}_2\text{C}$  have been measured in the presence of

(56) Kirmse, W.; Guth, M.; Steenken, S. *J. Am. Chem. Soc.* **1996**, *118*, 10838.

(57) Sujdak, R. J.; Jones, R. L.; Dorfman, L. M. *J. Am. Chem. Soc.* **1976**, *98*, 4875.

(58) As reported in ref 26. The authors did not specify the range of quencher concentrations used in acetonitrile, but the maximum concentration is presumably considerably below 1 M.

(59) Alkoxide ions have high mobilities due to the proton relay mechanism (Grothaus mechanism). Slower escape by the bulkier alkoxide ion derived from 2-propanol could be another reason that ion pair recombination is more important in this solvent than in the shorter alcohols.

(60) Gould, I. R.; Farid, S. *Acc. Chem. Res.* **1996**, *29*, 522.

(61) Agmon, N.; Szabo, A. *J. Chem. Phys.* **1990**, *92*, 5270.

(62) Shiota, H.; Pal, H.; Tominaga, K.; Yoshihara, K. *J. Phys. Chem.* **1996**, *100*, 14575.

(63) Pines, E.; Pines, D.; Barak, T.; Magnes, B. Z.; Tolbert, L. M.; Haubrich, J. E. *Ber. Bunsen-Ges. Phys. Chem.* **1998**, *102*, 511.

(64) Genosar, L.; Cohen, B.; Huppert, D. *J. Phys. Chem. A* **2000**, *104*, 6689.

(65) Cohen, B.; Huppert, D. *J. Phys. Chem. A* **2001**, *105*, 2980.

(66) Lima, J. C.; Abreu, I.; Brouillard, R.; Macanita, A. L. *Chem. Phys. Lett.* **1998**, *298*, 189.

(67) Alder, R. W.; Allen, P. R.; Williams, S. J. *J. Chem. Soc., Chem. Commun.* **1995**, 1267.

(68) Dixon, D. A.; Arduengo, A. J. *J. Phys. Chem.* **1991**, *95*, 4180.

proton donors in acetonitrile.<sup>5,56</sup> The observed rates were somewhat smaller than the diffusion limit, and the isotope effects were close to unity. It was argued that the lack of an isotope effect was due to a nonlinear transition-state geometry, or a rate-limiting preassociation step. In contrast to the results of Steenken and co-workers, we observe a kinetic isotope effect of 1.7 on protonation. This value is close to values observed for photoacids.<sup>63</sup>

The 9.0 ps time constant for protonation in methanol corresponds to a bimolecular rate of reaction of  $4.5 \times 10^9 \text{ M}^{-1} \text{ s}^{-1}$ . This rate is near the diffusion limit for methanol, but since photolysis occurs in the neat solvent the nascent carbene is surrounded by a number of potential proton donors, and no diffusion is necessary. In that sense, these experiments are the proton-transfer analogue of ultrafast intermolecular electron transfer where the solvent acts as electron donor.<sup>12,69,70</sup> Electron donation from a solvent can occur in  $< 100$  fs, but here proton donation requires significantly longer times. This indicates that a barrier exists to reaction—a barrier that we suggest arises from the solvent reaction coordinate.

The values of  $\tau_1$  support the notion that protonation of  ${}^1\text{Ph}_2\text{C}$  is limited by the time for the solvent to reorganize. The protonation of  ${}^1\text{Ph}_2\text{C}$  by an alcohol molecule creates an ion pair from two neutral species. It is therefore reasonable to expect that solvent fluctuations will be strongly coupled to the reaction coordinate, particularly since the solvent plays a dual role as proton donor and solvating medium. Many workers have emphasized the connection between solvation dynamics and proton transfer.<sup>71–74</sup> Solvent reorientation may be necessary before proton transfer can proceed.<sup>75</sup> Hynes and co-workers have suggested that solvent fluctuations are the reaction coordinate for nonadiabatic and adiabatic proton transfer.<sup>74</sup> Pines et al. have emphasized that exothermic intermolecular proton-transfer reactions are controlled by solvent fluctuations.<sup>63</sup> The protonation times reported here correlate reasonably well with solvation times of the various alcohols determined by Maroncelli and co-workers (see Table 2).<sup>76</sup> The correlation is not perfect, since the isotope effect of 1.7 is considerably larger than that observed for solvation in deuterated methanol. For intermolecular proton transfer to occur, it is believed that a hydrogen bond must first be formed between donor and acceptor.<sup>77</sup> In this case, the solvent must first form a hydrogen bond with the incipient carbene. In neat methanol, molecular dynamics simulations suggest that hydrogen bond lifetimes are  $\approx 5$  ps.<sup>78</sup> It is possible that this time increases in the deuterated solvent.

The bimolecular rate compares well with the value of  $5.6 \times 10^9 \text{ M}^{-1} \text{ s}^{-1}$  estimated by Eisenthal et al. for the reaction of  ${}^1\text{Ph}_2\text{C}$  with methanol in  $\text{N}_2$  saturated acetonitrile.<sup>18</sup> These authors measured a 1.6-fold slower rate of reaction for 2-propanol. The value of 35 ps from Table 2 and the molarity of neat 2-propanol

(13.1 M) gives a rate of  $2.2 \times 10^9 \text{ M}^{-1} \text{ s}^{-1}$ . This bimolecular rate is a factor of 2.0 slower than our measured rate in methanol. Eisenthal and co-workers also varied the concentration of methanol between 0 and 10 M in acetonitrile containing 0.1 M isoprene and measured the ratio of singlet to triplet products. From this independent measurement they derived a rate constant of  $7.4 \times 10^9 \text{ M}^{-1} \text{ s}^{-1}$  for the reaction of  ${}^1\text{Ph}_2\text{C}$  with methanol, corresponding to a lifetime of 5.5 ps in neat methanol. This is in reasonable agreement with our value of 9.0 ps.

These time constants must be compared cautiously with ours due to the variation in solvent. As seen with the carbocations, bimolecular reaction rates between singlet carbenes and alcohols increase with increasing alcohol concentration.<sup>5,56,79</sup> Kirmse et al. argued that the increased rates reflect the kinetic advantage of a second alcohol molecule which can stabilize the incipient alkoxide ion by hydrogen bonding.<sup>56</sup> Steenken observed increased bimolecular rates at increased alcohol concentration for carbenes reacting with weakly acidic alcohols.<sup>5</sup> This was attributed to more than one proton donor molecule participating in the protonation. These ideas are consistent with a rate-limiting role for the protic solvent.

**(5) Quantum Yield of Protonation.** According to the actinometric results in Figure 9, the quantum yield of  $\text{Ph}_2\text{CH}^+$ ,  $\phi_p$ , reaches a maximum value of 0.18, 18 ps after the pump pulse. Since  $\phi_p$  first increases, and then decreases, it is more useful to measure the fraction of all photoexcited diazo molecules that are ultimately protonated. This quantity, which we term the protonation fraction,  $f_p$ , is given by  $\phi_p/C_{\text{max}}$ .  $C_{\text{max}}$  is defined in eq 4 and is calculated from the time constants  $\tau_1$  and  $\tau_2$  determined by fitting. The value for methanol,  $f_p(\text{CH}_3\text{OH})$ , is equal to 0.30. If the relative signal amplitudes in Figure 8 are correct, then the protonation fraction in the other alcohols is given by

$$f_p = \frac{\Delta A_{\text{max}}}{\Delta A_{\text{max}}^{\text{CH}_3\text{OH}}} \cdot \frac{0.18}{C_{\text{max}}} \quad (5)$$

where  $\Delta A_{\text{max}}$  is the maximum absorbance change due to  $\text{Ph}_2\text{CH}^+$  in each alcohol. This assumes that the value of  $\epsilon$  at 435 nm is similar for  $\text{Ph}_2\text{CH}^+$  in all alcohols. Values of  $f_p$  are summarized in Table 2.

The protonation fraction decreases steadily on going from methanol to 2-propanol. In other words, fewer total carbocations are formed than are predicted from the rate constants of eq 2. This could be due to a decreased branching ratio for protonation in the less acidic alcohols. Belt et al. previously used nanosecond laser flash photolysis to estimate quantum yields of protonation for a series of diarylcarbenes in 1:1 TFE/acetonitrile.<sup>6</sup> They observed greater yields for longer-lived carbocations. Interestingly, the quantum yield for  $\text{Ph}_2\text{CH}^+$  in this solvent mixture was just 0.007. The quantum yields reported by Belt et al. cannot be primary yields since they were measured with nanosecond pulses. It is important to ask how many carbocations still remain several nanoseconds after the laser pulse. Even if the rate of reaction between TFE (a weak nucleophile) and  $\text{Ph}_2\text{CH}^+$  is low, the rate of the geminate reaction between the carbocation and the TFE anion could be much higher. We speculate that the low yields reported by Belt et al. are due to the fact that relatively few carbocations can escape these initial ion pairs.

- (69) Yoshihara, K. *Adv. Chem. Phys.* **1999**, *107* (Pt. 2), 371.  
 (70) Xu, Q.-H.; Scholes, G. D.; Yang, M.; Fleming, G. R. *J. Phys. Chem.* **1999**, *103*, 10348.  
 (71) Marcus, R. A. *Faraday Discuss. Chem. Soc.* **1982**, *74*, 7.  
 (72) Moog, R. S.; Maroncelli, M. *J. Phys. Chem.* **1991**, *95*, 10359.  
 (73) Mente, S.; Maroncelli, M. *J. Phys. Chem. A* **1998**, *102*, 3860.  
 (74) Ando, K.; Hynes, J. T. *Acid-Base Proton Transfer and Ion Pair Formation in Solution*; Advances in Chemical Physics; Wiley: New York, 1999; p 381.  
 (75) Kyrychenko, A.; Herbich, J.; Izydorzak, M.; Gil, M.; Dobkowski, J.; Wu, F. Y.; Thummel, R. P.; Waluk, J. *Isr. J. Chem.* **1999**, *39*, 309.  
 (76) Horng, M. L.; Gardecki, J. A.; Papazyan, A.; Maroncelli, M. *J. Phys. Chem.* **1995**, *99*, 17311.  
 (77) Eigen, M. *Angew. Chem., Int. Ed. Engl.* **1964**, *3*, 1.  
 (78) Matsumoto, M.; Gubbins, K. E. *J. Chem. Phys.* **1990**, *93*, 1981.

- (79) Griller, D.; Liu, M. T. H.; Scaiano, J. C. *J. Am. Chem. Soc.* **1982**, *104*, 5549.

It is not clear at this stage whether other reaction pathways are needed to explain the O–H insertion reaction. While the decreasing protonation fractions observed in the longer alcohols could be explained by increased branching into a concerted reaction pathway,<sup>6</sup> it could also be explained by less efficient formation of  $^1\text{Ph}_2\text{C}$  in these solvents. For example, if every third diazo excited state would form singlet carbene, then the total amount of  $\text{Ph}_2\text{CH}^+$  observed in methanol would be explained, assuming that protonation is the only decay channel. This is quite a bit below the photodestruction yield of 0.78 reported by Kirmse,<sup>45</sup> but, as discussed earlier, the initial quantum yield of  $^1\text{Ph}_2\text{C}$  is unknown. Although Kirmse argued that the photodecomposition quantum yield of  $\text{Ph}_2\text{CN}_2$  is independent of solvent,<sup>80</sup> his experiments measured only the net destruction rate of the diazo compound and do not provide any insight into how the carbene population might partition into different spin states. It is conceivable that partitioning of the initially excited diazo singlet state ( $^1\text{Ph}_2\text{CN}_2^*$  in Scheme 2) into  $^1\text{Ph}_2\text{C}$  and other states such as  $^3\text{Ph}_2\text{C}$  or  $^3\text{Ph}_2\text{C}^*$  could depend on solvent. Eisenthal showed that some amount of  $^3\text{Ph}_2\text{C}^*$  is formed in less than 20 ps after excitation at 266 nm.<sup>17</sup> Some evidence for lower primary quantum yields of  $^1\text{Ph}_2\text{C}$  in the longer alcohols comes from a comparison of the signals at 360 nm. When transients at 360 nm (data not shown) are plotted with the  $t = 0$  features scaled to have the same amplitude,<sup>81</sup> then the initial signal level at the conclusion of the spike decreases from methanol to 2-propanol. This suggests that less  $^1\text{Ph}_2\text{C}$  is formed immediately

after loss of  $\text{N}_2$ . Further studies are necessary before it can be decided whether every  $^1\text{Ph}_2\text{C}$  formed is ultimately protonated or whether reaction channels exist<sup>7</sup> that do not require protonation.

### Summary and Conclusions

The results presented here indicate that carbocations are short-lived intermediates when  $^1\text{Ph}_2\text{C}$  reacts in neat alcohols. Rates of protonation were measured directly and shown to correlate with solvation times in alcohols from methanol to 2-propanol. The rate-limiting step in the overall O–H insertion reaction is not protonation, but the decay of  $\text{Ph}_2\text{CH}^+$  by reaction with a nucleophile. In methanol and ethanol, ion pair collapse does not appear to compete with reaction of  $\text{Ph}_2\text{CH}^+$  with a neutral solvent molecule. In 2-propanol, however, the decay rate of the cation is faster than expected from the bimolecular reaction rate measured for 2-propanol at low concentration in acetonitrile. This is suggested to arise from geminate reaction in the initial ion pair. The ability to generate powerful bases on an ultrafast time scale opens up new possibilities for studying adiabatic proton-transfer reactions in polar solvents. For those carbenes with singlet ground states, which are also strong bases, it should be possible to study intermolecular proton-transfer reactions for which all participants are in their electronic ground states. This will simplify theoretical study of this important class of reactions.

**Acknowledgment.** We thank Professors Matthew S. Platz and Christopher M. Hadad of the Ohio State University for helpful comments.

JA017485R

(80) Kirmse, W. *Justus Liebigs Ann. Chem.* **1963**, 666, 9.

(81) The  $\text{CH}_3\text{OH}/\text{CH}_3\text{OD}$  data were recorded in back-to-back scans under identical experimental conditions. The spikes had the same amplitude, indicating no solvent isotope effect on this feature.